

EFFECTS OF CMAS APPLICATION ON THE ISOTHERMAL AND GRADIENT THERMAL CYCLING BEHAVIOR OF A $\text{Yb}_2\text{Si}_2\text{O}_7$ EBC

Michael J. Presby
NASA Glenn Research Center
Cleveland, OH, USA

Jamesa L. Stokes
NASA Glenn Research Center
Cleveland, OH, USA

Bryan J. Harder
NASA Glenn Research Center
Cleveland, OH, USA

John A. Setlock
The University of Toledo
Toledo, OH, USA

Jeffrey R. Hammel
Jacobs Technology
Cleveland, OH, USA

ABSTRACT

Environmental barrier coatings (EBCs) are critical to the continued advancement of gas turbine hot section materials technology. EBCs are required to protect Si-based ceramics such as silicon carbide fiber-reinforced silicon carbide (SiC/SiC) ceramic matrix composites (CMCs) from oxidation and corrosion in the combustion environment. One of the current challenges concerning EBC lifetime is the thermochemical reactions between calcium-magnesium-aluminosilicate (CMAS) deposits and the EBC that leads to changes in both composition and stress state. These changes can severely reduce the integrity of the EBC leading to crack formation, delamination, and spallation. Current techniques for evaluating CMAS in the laboratory rely on the pre-application of CMAS. Two commonly used application methods to deposit CMAS on EBC materials are tape-cast and air spray. In both methods, the CMAS is applied to the EBC surface at ambient temperature, and then subjected to a heat treatment process for binder burnout. The purpose of this study is to compare the tape-cast and air spray methods on the CMAS corrosion of a ytterbium disilicate ($\text{Yb}_2\text{Si}_2\text{O}_7$) EBC exposed to isothermal, and gradient thermal cycling. The results highlight if any differences exist in the CMAS infiltration kinetics between the two application methods.

Keywords: Environmental barrier coatings (EBCs); Environmental durability; Calcium-magnesium-aluminosilicate (CMAS).

1. INTRODUCTION

Improvements in the efficiency of gas turbine engines is enabled by the implementation of hot-section hardware fabricated using silicon carbide (SiC)-based ceramic matrix

composites (CMCs) [1]. CMCs have a higher temperature capability and lower density compared to traditionally used nickel-based superalloys [1]. However, SiC-based CMCs are susceptible to severe degradation due to thermochemical reactions with water vapor that is generated as a by-product of combustion [2-3]. The deleterious interactions with water vapor led to the development of environmental barrier coatings (EBCs) to protect SiC-based CMCs to meet the durability and life required for use as engine components.

In addition to having good water vapor resistance, EBCs must also be able to withstand other environmentally induced damage mechanisms such as thermomechanical stress, solid particle erosion (SPE), foreign object damage (FOD), and calcium-magnesium-aluminosilicate (CMAS) attack [3].

As engine operating temperatures continue to increase, the vulnerability of EBCs to attack by molten silicate deposits (CMAS) becomes an inescapable challenge [4-5]. Above $\sim 1,200^\circ\text{C}$, siliceous debris such as desert sand, volcanic ash, and other mineral dust ingested into the engine can become partially or completely molten, deposit on engine components, and deleteriously react with coatings or substrates. The reactions of CMAS with EBCs can lead to the formation of extrinsic phases, coating consumption, and the overall loss of mechanical integrity [4-10].

Understanding the effects of CMAS on the degradation of EBCs is inherently complex. There exists a wide range of silicate deposit compositions that vary depending upon region [5]. The composition, and operating temperature can strongly affect the melting, infiltration, and reaction kinetics. While protocols for selecting CMAS compositions have been proposed [5], and many researchers and OEMs have adopted the use of ‘standard’ compositions based on engine hardware observations to enable

comparative studies [11], many labs still incorporate different techniques during testing. This includes the method of CMAS application (tape-cast versus air spray) [9, 12-15], test environment (furnace [11-15], laser [16], burner/combustion rig [9, 17-20]), and the test method (isothermal [11-15], thermal gradient [16-18], static [11-15], cycling [16-18]). While different techniques have been incorporated among various studies, there are few systematic investigations comparing different methods/techniques to determine if, and how test results are affected. As such, the purpose of this study is to compare two common application methods for depositing CMAS: tape-cast and air spray. For both methods, EBC samples are subject to isothermal, and gradient thermal cycling to see if any differences exist in the CMAS infiltration kinetics between the two application methods.

2. MATERIALS AND METHODS

The material system used in this work was a ytterbium disilicate ($\text{Yb}_2\text{Si}_2\text{O}_7$) EBC with a silicon (Si) bond coat. The coatings were deposited via air plasma spray (APS) onto 25.4 mm diameter by 3 mm thick α -SiC (Hexoloy SA®, Saint Gobain) substrates. Prior to deposition, the substrates were grit blasted with cubic boron nitride (CBN) powder to an average roughness (R_a) of $\sim 6 \mu\text{m}$. The Si bond coat thickness was $\sim 125 \mu\text{m}$ and the $\text{Yb}_2\text{Si}_2\text{O}_7$ topcoat thickness was $\sim 300 \mu\text{m}$. The deposition conditions are proprietary, but consistent with those reported in previous publications [21]. The porosity of the as-sprayed coatings was estimated to be 5.5%.

The CMAS composition used in this study consisted of 30.67 mol% CaO, 8.25 mol% MgO, 12.81 mol% $\text{AlO}_{1.5}$, and 48.27 mol% SiO_2 . This composition is based off the chemistry of deposits found on turboshaft shrouds operated in a desert environment [11]. This composition has been used in other studies [9,11,15] and exhibits congruent melting with a melting point of $\sim 1,240^\circ\text{C}$.

CMAS was applied to the surface of the EBCs using a tape-cast and air spray method. Both methods have been used in previous studies [14-15]. For the tape-cast method, a CMAS slurry was prepared by ball milling 58.5 wt.% CMAS powder with 1.2 wt.% menhaden fish oil, 20.3 wt.% xylene, 13.6 wt.% ethanol, 4.1 wt.% polyvinyl butyral binder, and 2.3 wt.% benzyl phthalate plasticizer. Circular tapes of 22.23 mm were applied to the EBC surface with a target loading of $\sim 8 \text{ mg/cm}^2$.

For the air spray method, a solution of 36.9 wt.% CMAS powder, 21.8 wt.% alpha terpineol, 35.6 wt.% xylene, 1.1 wt.% ethyl cellulose, 4.2 wt.% methanol, and 0.4 wt.% oleic acid was prepared. The alpha terpineol and xylene acted as solvent carriers while the ethyl cellulose acted as a binder to help the CMAS solution adhere to the EBC surface. The liquid solution was sprayed onto the EBC surface using an airbrush. Similar to the tape cast samples, the target loading was $\sim 8 \text{ mg/cm}^2$.

The tape-cast and air spray samples were subjected to an initial heat treatment to burn off the organics. The samples were heated up to 420°C at a rate of 0.2°C/min , held at temperature for 2 hours, and then cooled back to room temperature at 1°C/min .

After the binder burn out, all samples underwent a heat treatment at $1,316^\circ\text{C}$ for 30 min with 10°C/min heating and 20°C/min cooling to initially melt and react the CMAS. After this initial melt, samples were subject to either an isothermal heat treatment in a furnace, or gradient thermal cycling using a laser.

For the isothermal heat treatment in the furnace, samples were subject to 25- and 50-hour heat treatments at $1,316^\circ\text{C}$ at 10°C/min heating and cooling.

Gradient thermal cycling was performed using a 4,000-Watt carbon dioxide (CO_2) laser. The EBC surface temperature was $1,316^\circ\text{C}$ with a 60 sec ramp, a 30 min hold, and then a 5 min cooling cycle where the laser shutter was closed and the sample was allowed to cool back to room temperature. The backside of the sample was subject to free convection at ambient temperature (i.e., no forced cooling air), which corresponded to a backside surface temperature of $1,093^\circ\text{C}$. The EBC surface temperature was monitored with a pyrometer with a spectral range of $7.6 - 8.3 \mu\text{m}$, and the backside temperature was monitored with a two-color pyrometer with two spectral bands: one at $0.7 - 1.1 \mu\text{m}$ and one at $1.0 - 1.1 \mu\text{m}$. Samples were subjected to 50 and 100 cycles, corresponding to 25 and 50 hot hours, respectively: the same total “hot” duration as the isothermal samples. A schematic of the laser test setup is shown in Figure 1. The beam exiting the laser head has a Gaussian profile as shown in Figure 2a. To uniformly heat the EBC surface, a zinc selenide (ZnSe) transmissive faceted lens is used to create a beam profile with a relatively flat intensity profile as shown in Figure 2b. While the ZnSe lens creates a square profile, the lens is configured into a boring head that provides rotation to the lens creating an optically circular profile.

Post testing, samples were cross-sectioned, mounted, and polished to analyze the infiltration and damage using scanning electron microscopy (SEM).

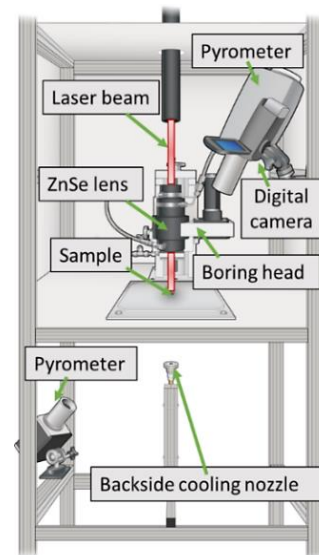


FIGURE 1: SCHEMATIC OF LASER GRADIENT THERMAL CYCLING TEST SETUP.

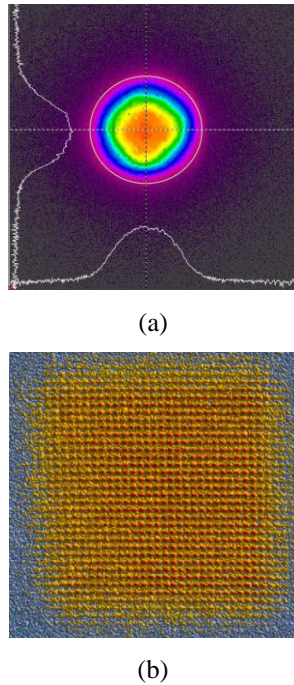


FIGURE 2: BEAM PROFILE (A) GAUSSIAN, (B) SQUARE FOCUS WITH FLAT INTENSITY OBTAINED USING ZINC SELENIDE TRANSMISSIVE FACETED LENS.

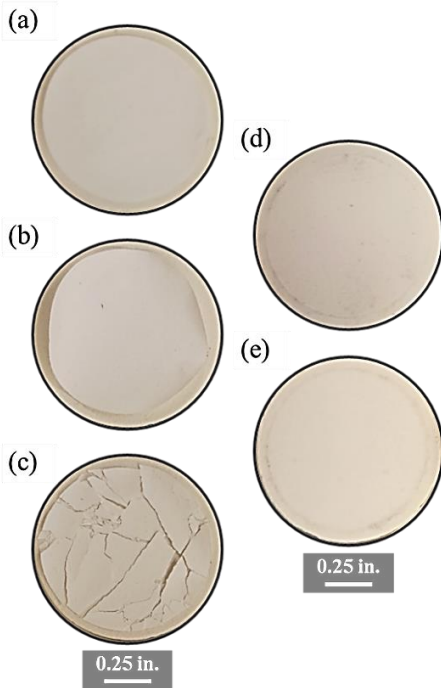


FIGURE 3: OPTICAL IMAGES OF TAPE-CAST SAMPLES (A) BEFORE HEAT TREATMENT, (B) AFTER HEAT TREATMENT AT 420°C FOR 2 HOURS, (C) AFTER PRESSING DOWN HEAT-TREATED TAPES TO MAKE FLAT. (D) AND (E) REPRESENT AIR SPRAY SAMPLES BEFORE AND AFTER HEAT TREATMENT AT 420°C FOR 2 HOURS, RESPECTIVELY.

3. RESULTS AND DISCUSSION

3.1 Organics burn off and initial melt

The CMAS tape was applied flat to each sample as shown in Figure 3a. However, upon heat treatment to 420°C to burn off the organic fillers, the tapes curled up from the edges as shown in Figure 3b. The curled-up tapes were susceptible to cracking when attempting to press them down to lie flat for uniform coverage, as displayed in Figure 3c, resulting in gaps in the tape.

Conversely, the air spray samples (Figures 3d and 3e) maintained better adherence to the coating surface and did not exhibit any deformation or lifting during the 420°C heat treatment.

Figure 4 shows optical images of tape-cast (Figure 4a) and air spray (Figure 4b) witness samples after the initial melt heat treatment at 1,316°C for 30 min. For the tape-cast samples, it was evident that residual CMAS bubbles (outlined by dashed circles in Figure 4a) remained on the surface. Conversely, glassy regions were observed on the surface of the air spray samples (outlined by a dashed circle in Figure 4b) but the CMAS was generally more dispersed across the surface and did not bead up or form bubbles as in the tape-cast samples.

Representative SEM micrographs of cross sections of the tape-cast and air spray samples are displayed in Figure 4c and Figure 4d, respectively. Both application methods resulted in an interaction layer consisting of apatite grains near the surface of the coatings. Additionally, CMAS was observed to infiltrate the entire thickness of the coatings for both application methods as evidenced by CMAS pockets observed between grains near the

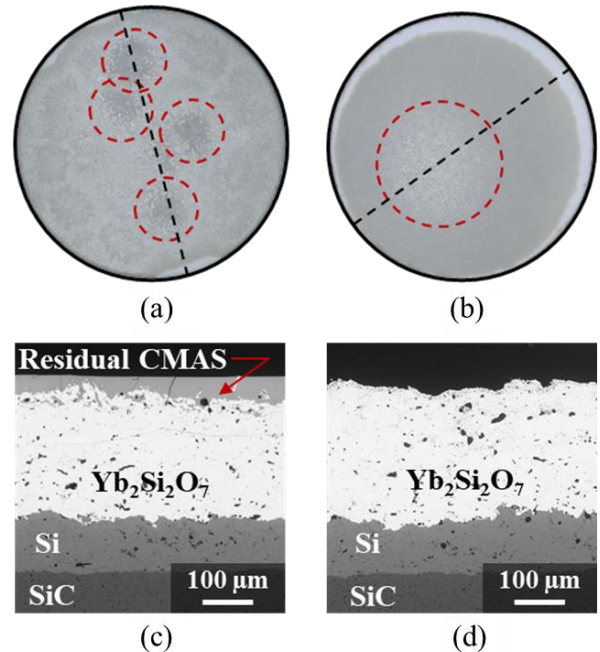


FIGURE 4: OPTICAL IMAGES OF (A) TAPE-CAST AND (B) AIR SPRAY WITNESS SAMPLES AFTER HEAT TREATMENT AT 1,316°C FOR 30 MIN. SEM MICROGRAPHS OF (C) TAPE-CAST AND (D) AIR SPRAY WITNESS SAMPLES AFTER HEAT TREATMENT AT 1,316°C FOR 30 MINUTES. THE DASHED LINE INDICATES CROSS SECTION PLANE.

bond coat. The overall morphology of the coatings did not differ significantly between the two application methods, as pockets of CMAS were dispersed throughout the coatings and grain coarsening was observed. The main difference observed was the tendency for the tape samples to have a larger amount of residual CMAS remaining on the surface above the apatite grains corresponding to the glass bubbles observed on the surface. There was some cracking observed in the residual CMAS that also appeared to extend through the interaction region in several areas across the coating. This cracking is likely due to CTE mismatch between the residual CMAS glass and the underlying EBC material upon cooling [3, 22].

3.2 Isothermal

Figure 5 shows SEM micrographs of sample cross sections tested in an isothermal environment for 25 hours at 1,316°C. As shown in Figures 5a and 5b, the tape-cast method resulted in pockets of CMAS, formation of large pores and voids, grain coarsening, crack formation near the coating surface, and delamination at the bond coat – topcoat interface. As evident in Figure 5b, the CMAS penetrated through the entire thickness of the $\text{Yb}_2\text{Si}_2\text{O}_7$ topcoat resulting in a weakened interface and subsequent delamination. A similar coating/damage morphology showing pockets of CMAS, formation of large pores and voids, grain coarsening, crack formation, and delamination is presented in Figures 5c and 5d for the air spray method. This highlights that the two application methods yielded comparable results in both damage and depth of CMAS infiltration.

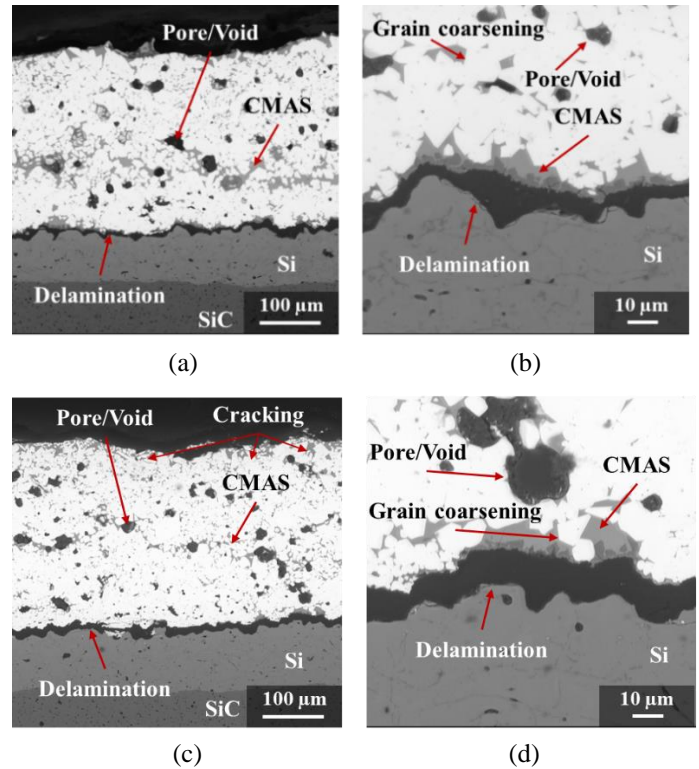


FIGURE 6: SEM MICROGRAPHS FROM ISOTHERMAL TESTING FOR 50 HOURS AT 1,316°C: (A) AND (B) TAPE-CAST, (C) AND (D) AIR SPRAY.

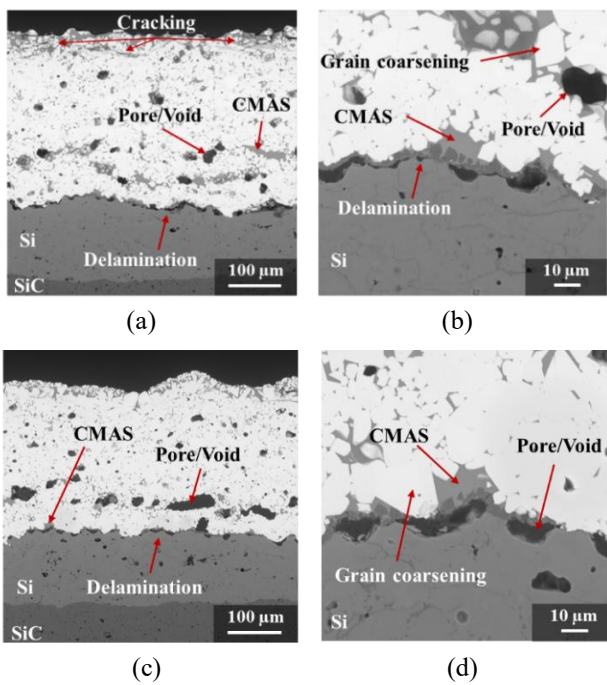


FIGURE 5: SEM MICROGRAPHS FROM ISOTHERMAL TESTING FOR 25 HOURS AT 1,316°C: (A) AND (B) TAPE-CAST, (C) AND (D) AIR SPRAY.

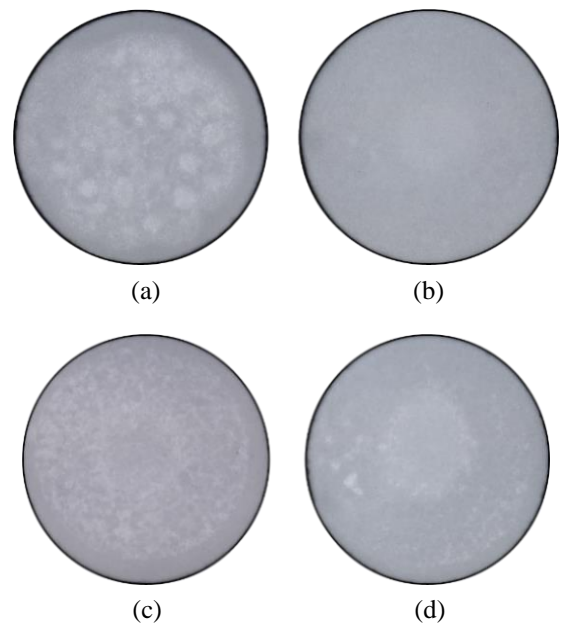


FIGURE 7: OPTICAL IMAGES OF TAPE-CAST (A) 25 HOUR, (B) 50 HOUR, AND AIR SPRAY (C) 25 HOURS AND (D) 50 HOURS TESTED IN AN ISOTHERMAL ENVIRONMENT AT 1,316°C.

Figure 6 displays representative cross-sections of samples tested for 50 hours in an isothermal environment at 1,316°C. Analogous to the 25-hour isothermal heat treatment, the coating/damage morphology after 50 hours showed pockets of CMAS throughout the entire thickness of the $\text{Yb}_2\text{Si}_2\text{O}_7$ topcoat, formation of large pores and voids, crack formation near the coating surface, and grain coarsening. While delamination at the bond coat – topcoat interface was also observed in both the 25-hour and 50-hour isothermal tests, the extent of delamination after 50 hours was more severe highlighting a further reduction in the integrity of the interface as exposure duration increased. This underscores the importance of understanding environmental effects on EBC adhesion/interfacial strength [23] since this will be a life-limiting failure mode.

For both the 25- and 50-hour isothermal tests, the CMAS appeared to completely infiltrate the coating with no evidence of residual glass on the surface as shown by the optical images in Figure 7.

3.3 Gradient thermal cycling

Representative cross-sections of samples tested under gradient thermal cycling conditions with an EBC surface temperature of 1,316°C and backside SiC substrate temperature of 1,093°C are shown in Figure 8. Due to the presence of a thermal gradient, most of the CMAS infiltration was contained to approximately the upper two-thirds of the $\text{Yb}_2\text{Si}_2\text{O}_7$ topcoat marked by the dashed lines. Additional cross-sectional images with energy dispersive X-ray spectroscopy (EDS) mapping are

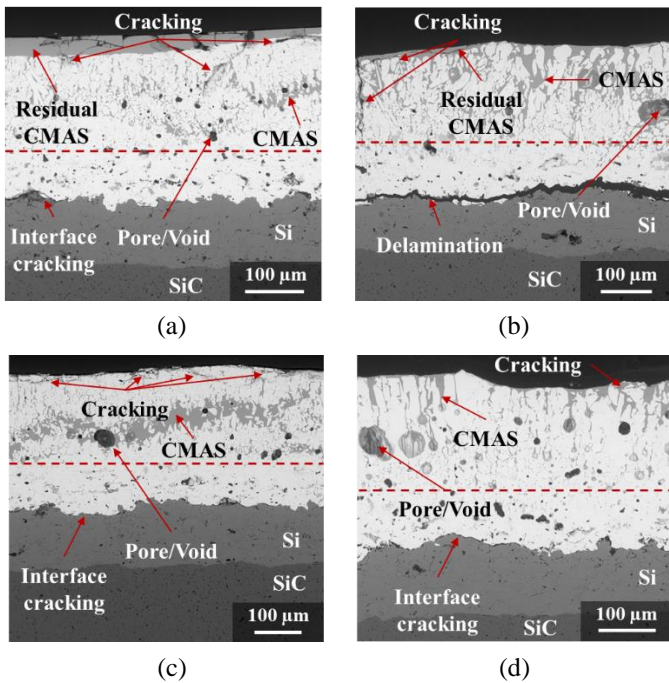


FIGURE 8: SEM MICROGRAPHS FROM GRADIENT THERMAL CYCLING AT 1,316°C: TAPE-CAST (A) 25 HOURS AND (B) 50 HOURS, AND AIRSPRAY (C) 25 HOURS AND (D) 50 HOURS.

shown in Figure 9 to highlight the differences observed in the infiltration between isothermal and gradient thermal cycling. For the isothermally tested samples, CMAS was more dispersed through the entire thickness of the coating, with much of the CMAS reacting and forming apatite. On the other hand, the EDS maps highlight the large bands of calcium (Ca) deposits observed in the gradient thermal cycling samples designated by the dashed white lines in Figure 9(b) and 9(d).

Cracking in the $\text{Yb}_2\text{Si}_2\text{O}_7$ topcoat surface was also observed, similar to the isothermally tested samples; however, the extent of cracking appeared to be more severe with coating loss occurring in some areas as shown by the cross-sections in Figure 10. In addition, some residual CMAS could also be observed on the surface as shown by the optical images in Figure 11. Both the

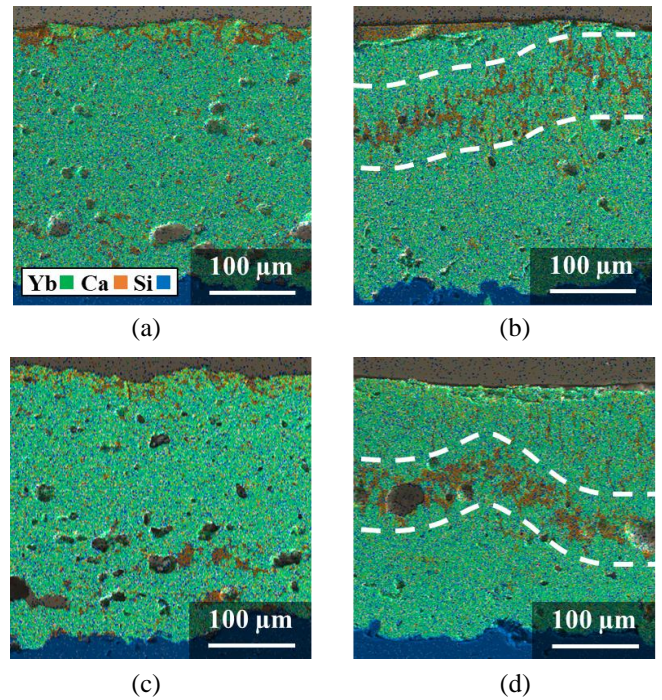


FIGURE 9: EDS MAPS OF TAPE-CAST (A) ISOTHERMAL, (B) GRADIENT THERMAL CYCLING, AND AIR SPRAY (C) ISOTHERMAL, (D) GRADIENT THERMAL CYCLING.

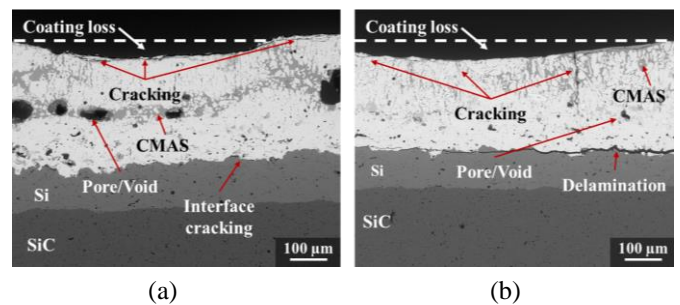


FIGURE 10: SEM MICROGRAPHS FROM GRADIENT THERMAL CYCLING AT 1,316°C (A) 25 HOURS AIR SPRAY AND (B) 50 HOURS TAPE-CAST.

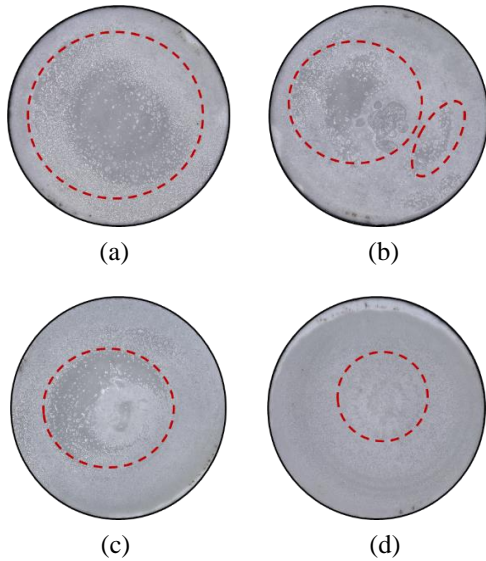


FIGURE 11: OPTICAL IMAGES OF TAPE-CAST (A) 25 HOURS (B) 50 HOURS, AND AIR SPRAY (C) 25 HOURS AND (D) 50 HOURS TESTED IN GRADIENT THERMAL CYCLING CONDITIONS. GLASSY REGIONS (RESIDUAL CMAS) OUTLINED WITH DASHED CIRCLES.

tape-cast and air spray samples exhibited some residual CMAS on the surface which tended to decrease as the time at temperature increased from 25 to 50 hours.

The 25-hour gradient thermal cycling samples exhibited some minor cracking at the bond coat – topcoat interface which contrasts with the widespread delamination observed in the isothermally tested samples. The 50-hour gradient thermal cycling samples exhibited increased cracking and delamination at the bond coat – topcoat interface which was more comparable to the extent observed in the isothermal samples. The increased time to observe a similar degree of delamination in the thermal gradient cycling samples is likely due to cooler interface temperature (estimated to be $\sim 1,175 - 1,200^{\circ}\text{C}$) which minimizes CMAS infiltration down to the bond coat and reduces the deleterious reactions that weaken the interface. An interface temperature of $\sim 1,175 - 1,200^{\circ}\text{C}$ is below the melting point of the CMAS used in the work ($\sim 1,240^{\circ}\text{C}$). Increasing the EBC surface temperature, and correspondingly the interface temperature, would lead to different observations as CMAS infiltration, reactivity, and damage should increase. Furthermore, changing the thermal gradient, heating/cooling rates, and cycle time/frequency can influence damage progression. Further work is warranted to understand how these variables will influence EBC degradation over time.

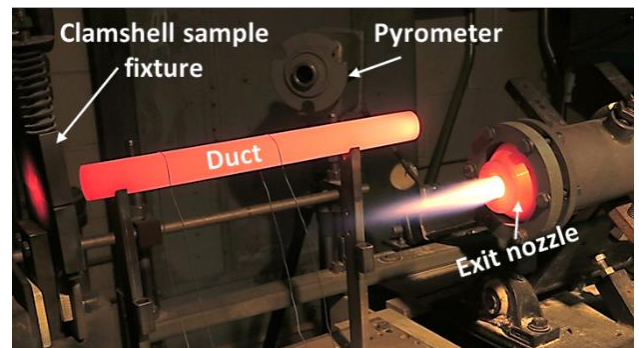
4. IMPLICATIONS AND FUTURE WORK

In service, engine hardware will be subject to thermal gradients and go through multiple engine cycles (heating and cooling). As such, the observations from this work demonstrate the need to perform CMAS testing under relevant conditions

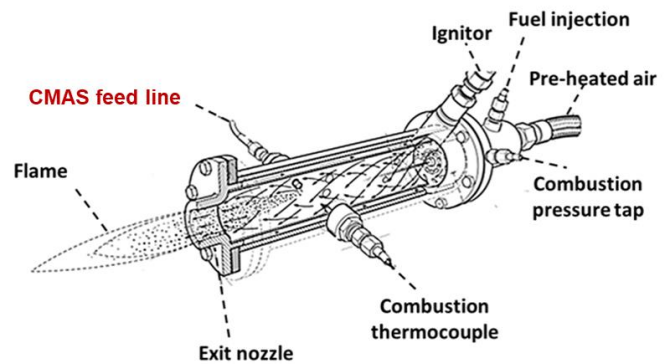
(i.e., thermal gradients and cycling) to ensure the appropriate damage modes are generated during laboratory scale testing as would be observed in service. This is particularly true when attempting to develop life-prediction models. In addition, it is crucial to understand how the method of testing influences the observed results. Despite the differences observed between test methods (isothermal vs. gradient thermal cycling), the CMAS application method (tape-cast vs. air spray) does not appear to significantly influence the infiltration or damage features irrespective of test method. However, CMAS deposited via the air spray method appears to adhere better to the coating surface during the initial heat treatment when burning off the organics.

Nonetheless, the tape-cast and air spray are ‘static’ application methods where the CMAS is applied at ambient temperature before exposing to high temperature environment. However, in service, CMAS deposition is a dynamic process where CMAS will gradually accrue over time at elevated temperatures. As a result, there is a strong need to develop more dynamic approaches for CMAS testing.

Throughout their life, hot-section materials will exhibit erosion, deposition, and corrosion depending upon the composition of particles and operating conditions of the engine. As such, a more realistic approach is to develop a method where



(a)



(b)

FIGURE 12: BURNER RIG CONFIGURATION. (A) BURNER RIG EXIT NOZZLE, UNATTACHED DUCT, CLAMSHELL SAMPLE FIXTURE, AND PYROMETER. (B) SCHEMATIC OF THE BURNER RIG PLACED BEFORE THE DUCT HIGHLIGHTING THE LOCATION OF THE CMAS FEED LINE.

CMAS is deposited in a combustion environment [17-20]. Some facilities have already developed and shown the feasibility of performing dynamic CMAS testing for TBCs [17-18] and EBCs [19-20]. Consequently, investigations are being performed using a jet-fueled burner rig at NASA Glenn Research Center, shown in Figure 12, for short and long duration (minutes to hundreds of hours) CMAS erosion, deposition, and corrosion studies. In this facility, CMAS particles can be gradually introduced under different operating regimes while materials are exposed to the high temperature, cyclic environment that gas turbine hot-section components encounter during their lifetime. Preliminary CFD modeling has shown that CMAS particles injected into the burner rig become molten by the time they impinge on the sample surface [20].

The results presented in this work will also serve as a comparison to the dynamic method [24] in the burner rig to support our further understanding of CMAS degradation of EBCs and to understand if and how different test methods can influence damage initiation and progression. This will assist in ensuring that test methodologies are adequate for characterizing the effects of CMAS corrosion. Lastly, it must be noted that additional characterization after CMAS exposure is also warranted, specifically to understand how the mechanical properties (modulus, fracture toughness, etc.) of the EBC changes due to CMAS corrosion. This will be required to understand the durability of the EBC system and to develop more accurate life prediction models.

5. CONCLUSION

Two methods of applying CMAS, tape-cast and air spray, were compared under isothermal and gradient thermal cycling conditions to determine if the method of CMAS application has any effect on the CMAS infiltration and damage features. While the air spray method initially adhered better to the EBC surface during and after the organics burn off, no significant differences in infiltration or damage features could be observed after the 25- and 50-hour isothermal and gradient thermal cycling tests when compared on the basis of the application method.

While the method of CMAS application did not influence the infiltration or observed damage, there were differences in damage morphology between the isothermal and gradient thermal cycling tests. In the isothermal tests, the CMAS had more widespread infiltration through the EBC and down to the Si bond coat causing significant delamination. In contrast, CMAS infiltration for the thermal gradient tested samples was primarily contained to the upper two-thirds of the EBC where large calcium (Ca) deposits were observed. Due to the thermal gradient and cooler interface temperature (~1,175 – 1,200°C), CMAS infiltration and reactivity was reduced at the bond coat – topcoat interface. As a result, the extent of delamination in the gradient thermal cycling samples was less than the isothermally tested samples. These results support the importance of testing under relevant conditions (i.e., temperatures and thermal gradients) to ensure the appropriate damage modes are observed during laboratory testing as would be expected during operation.

ACKNOWLEDGEMENTS

The authors would like to acknowledge the Hybrid Thermally Efficient Core (HyTEC) and Transformation Tools and Technologies (TTT) projects for support of this work.

REFERENCES

- [1] Zok, F., 2016, "Ceramic-matrix composites enable revolutionary gains in turbine engine efficiency," *Am. Ceram. Soc. Bull.*, **95**(5), pp. 22-28.
- [2] Lee, K.N., van Roode, M., 2019, "Environmental barrier coatings enhance performance of SiC/SiC ceramic matrix composites," *Am. Ceram. Soc. Bull.*, **98**(3), pp. 46-53.
- [3] Lee, K.N., Zhu, D., Lima, R.S., 2021, "Perspectives on environmental barrier coatings (EBCs) manufactured via air plasma spray (APS) on ceramic matrix composites (CMCs): a tutorial paper," *J. Therm. Spray Technol.*, **30**, pp. 40-58.
- [4] Poerschke, D.L., Jackson, R.W., Levi, C.G., 2017, "Silicate deposit degradation of engineered coatings in gas turbines: progress toward models and materials solutions," *Ann. Rev. Mater. Res.*, **47**, pp. 297-330.
- [5] Ericks, A.R., Zok, F.W., Poerschke, D.L., Levi, C.G., 2022, "Protocol for selecting exemplary silicate deposit compositions for evaluating thermal and environmental barrier coatings," *J. Am. Ceram. Soc.*, **105**(6), pp. 3665-3688.
- [6] Harder, B.J., Ramirez-Rico, J., Almer, J.D., Lee, K.N., Faber, K.T., 2011, "Chemical and mechanical consequences of environmental barrier coating exposure to calcium-magnesium-aluminosilicate," *J. Am. Ceram. Soc.*, **94**(S1), pp. S178-S185.
- [7] Stokes, J.L., Harder, B.J., Wiesner, V.L., Wolfe, D.E., 2020, "Effects of crystal structure and cation size on molten silicate reactivity with environmental barrier coating materials," *J. Am. Ceram. Soc.*, **103**(1), pp. 622-634.
- [8] Stokes, J.L., Harder, B.J., Wiesner, V.L., Wolfe, D.E., 2019, "High-Temperature thermochemical interactions of molten silicates with Yb₂Si₂O₇ and Y₂Si₂O₇ environmental barrier coating materials," *J. Eur. Ceram. Soc.*, **39**(15), pp. 5059-5067.
- [9] Stokes, J.L., Presby, M.J., Webster, R.I., Setlock, J., Harder, B.J., 2023, "Thermochemical/thermomechanical synergies of high-temperature solid particle erosion of CMAS-exposed EBCs," *Proc. ASME Turbo Expo 2023*, Boston, MA, June 26-30, 2023, GT2023-101212.
- [10] Padture, N.P., 2019, "Environmental degradation of high-temperature protective coatings for ceramic-matrix composites in gas-turbine engines," *npj Mater. Degrad.*, **3**(11).
- [11] Kramer, S., Yang, J., Levi, C.G., Johnson, C.A., 2006, "Thermochemical interaction of thermal barrier coatings with molten CaO-MgO-Al₂O₃-SiO₂ (CMAS) deposits," *J. Am. Ceram. Soc.*, **89**(10), pp. 3167-3175.
- [12] Grant, K.M., Kramer, S., Lofvander, J.P.A., Levi, C.G., 2007, "CMAS degradation of environmental barrier coatings," *Surf. Coat. Tech.*, **202**, pp. 653-657.

- [13] Sleeper, J., Garg, A., Wiesner, V.L., Bansal, N.P., 2019, "Thermochemical interactions between CMAS and $\text{Ca}_2\text{Y}_8(\text{SiO}_4)_6\text{O}_2$ apatite environmental barrier coating material," *J. Eur. Ceram. Soc.*, **39**(16), pp. 5380-5390.
- [14] Kowalski, B., Stokes, J., Albert, P.E., Lauer, P.E., Wolfe, D.E., 2023, "Effect of test parameters in the exposure of Ca-Mg-Al-silicate on yttria stabilized zirconia," *J. Am. Ceram. Soc.*, **106**(6), pp. 3911-3921.
- [15] Harder, B.J., Stokes, J.L., Kowalski, B.A., Stuckner, J., Setlock, J.A., 2023, "Steam oxidation performance of $\text{Yb}_2\text{Si}_2\text{O}_7$ environmental barrier coatings exposed to CMAS," *J. Eur. Ceram. Soc.*
- [16] Jackson, R.W., Zaleski, E.M., Poerschke, D.L., Hazel, B.T., Begley, M.R., Levi, C.G., 2015, "Interaction of molten silicates with thermal barrier coatings under temperature gradients," *Acta Materialia*, **89**, pp. 396-407.
- [17] Mack, D.E., Wobst, T., Ophelia D. Jarligo, M., Sebold, D., Vaben, R., 2017, "Lifetime failure modes of plasma sprayed thermal barrier coatings in thermal gradient rig tests with simultaneous CMAS injection," *Surf. Coat. Tech.*, **324**, pp. 36-47.
- [18] Gildersleeve, E., Viswanathan, V. Sampath, S., 2019, "Molten silicate interactions with plasma sprayed thermal barrier coatings: role of materials and microstructure," *J. Eur. Ceram. Soc.*, **39**, pp. 2122-2131.
- [19] Okita, Y., Suzuki, M., Yamane, T., Hasegawa, J., Mizokami, Y., Nakamura, T., 2022, "Effect of temperature and velocity on microparticle erosion/deposition into environmental-barrier-coated ceramic matrix composite for aeroengines," *ASME J. Turbomach.* **144**(12), 121014.
- [20] Miller, R.A., Kuczmarski, M.A., 2015, "A CFD-based study of the feasibility of adapting an erosion burner rig for examining the effect of CMAS deposition/corrosion on environmental barrier coatings," NASA/TM-2015-218757, ntrs.nasa.gov.
- [21] Lee, K.N., 2019, " $\text{Yb}_2\text{Si}_2\text{O}_7$ Environmental barrier coatings with reduced bond coat oxidation rates via chemical modifications for long life," *J. Am. Ceram. Soc.* **102**(3), pp. 1507-1521.
- [22] Wiesner, V.L., Bansal, N.P., 2015, "Mechanical and thermal properties of calcium-magnesium aluminosilicate (CMAS) glass," *J. Euro. Ceram. Soc.* **35**(10), pp. 2907-2914.
- [23] Harder, B.J., Presby, M.J., Salem, J.A. Arnold, S.M., Mital, S.K., "Environmental barrier coating oxidation and adhesion strength," *ASME J. Eng. Gas Turbines Power*, **143**(3), 031004.
- [24] Stokes, J.L., Presby, M.J., "A Dynamic Testing Approach for Particulate Erosion-Corrosion for Gas Turbine Coatings," *Proc. ASME Turbo Expo 2024*, London, England United Kingdom, June 24-28, 2024. GT2024-121703.